Biosensors and Bioelectronics 52 (2014) 111–117

Contents lists available at ScienceDirect

Biosensors and Bioelectronics

journal homepage: www.elsevier.com/locate/bios

Highly electrostatically-induced detection selectivity and sensitivity for a colloidal biosensor made of chitosan nanoparticle decorated with a few bare-surfaced gold nanorods

Ren-Der Jean [a], Wei-Da Cheng [a], Meng-Hsuan Hsiao [a,b], Fu-Hsuan Chou [a], Jong-Shing Bow [c], Dean-Mo Liu [a,*]

[a] Department of Materials Science and Engineering, National Chiao Tung University, Hsinchu, Taiwan, ROC
[b] Material and Chemical Research Laboratories, Industrial Technology Research Institute, Hsinchu, Taiwan, ROC
[c] Center for Micro/Nano Science and Technology, National Cheng Kung University, Taiwan, ROC

ARTICLE INFO

Article history:
Received 12 June 2013
Received in revised form
21 August 2013
Accepted 22 August 2013
Available online 30 August 2013

Keywords:
Biosensor
Electrostatic interaction
Gold nanorod
Selectivity
Human serum albumin
Lysozyme

ABSTRACT

Metallic nanoparticles have been utilized as an analytical tool to detecting a wide variety of organic analytes. Among them, gold nanoparticles demonstrating outstanding surface plasmonic resonance property have been well recognized and received wide attention for plasmon-based sensing applications. However, in literature, gold-based nanosensor has to be integrated with specific "ligand" molecule in order to gain molecular recognition ability. However, "ligand" molecules, included proteins, peptides, nucleic acids, etc. are expensive and vulnerable to environmental change, in the meantime, anchoring procedure of the "ligand" molecules to gold surface may be cost-ineffective and endangered to the ligand 's activity, making a final analytic probe less reliable and risk in production capability. Here, we develop a new approach by designing a colloid-type sensor using a few "bare" Au nanorods deposited on the surface of a colloidal chitosan carrier. By tuning the solution pH, the resulting colloidal nanoprobe is capable of detecting proteins, i.e., human serum albumin and lysozyme, with high specificity and sensitivity. This new approach allows a new type of the molecular probes to be well manipulated to monitor important biomolecules for medical detection, diagnosis, and bioengineering applications.

1. Introduction

Development in sensing technologies has received enormous attention in recent decades due in part to the advancement in nanomaterials technology (Kim and Kang, 2008; Lei and Ju, 2012; Doria et al., 2012; Chen and Chatterjee, 2013) and in part, an urgent demand arising from the awareness of both environmental issue and in particular, healthcare concern. For healthcare, early-phase diagnosis of disease progression in human society promises better therapeutic strategy to be performed practically. To achieve a precise and efficient diagnosis, an important goal in biosensor evolution is to produce nanoscale assemblies capable of continuously monitoring concentrations of a specific analyte in a simple, reliable, highly-sensitive, and highly-specific manner. Therefore, designing biosensors with higher efficiency depends on the development of novel materials with considerable improvement in the recognition efficiency and ability for the binding event.

In recent years, a variety of nanoparticles, predominately gold nanoparticles and carbon nanotube, have been applied as the labels in nanoparticle-based amplification platforms which can dramatically enhance the signal intensity for a number of biosensors, such as electrochemical immunosensors, and lead to ultrasensitive bioassays (Yu et al., 2006; Cui et al., 2008; De et al., 2008; Wu et al., 2009). In general, biosensors hold two functional features: (1) a recognition capability to which a selective/specific binding toward target analytes is designed and (2) a transducer element for signaling the binding event. An efficient biosensor relies strongly upon these two functional features in order to achieve a recognition process in terms of response time, signal-to-noise (S/N) ratio, selectivity, and limits of detection (LOD). A vast number of technical publications reported in recent decade disclosed that materials with nanometric length feature unique physicochemical properties that can be of great opportunity in creating new recognition processes for chemical and biological sensors (Iqba et al., 2000; Venkata, 2012; Saha et al., 2012; Tansil and Gao, 2006). The utilization of gold nanoparticle (i.e. AuNP) as a sensory element has brought a broad spectrum of innovative approaches for the detection of metal ions, small molecules, proteins, nucleic acids, malignant cells, etc., in a rapid and efficient

* Corresponding author.
E-mail address: deanmo_liu@yahoo.ca (D.-M. Liu).

0956-5663/$ - see front matter © 2013 Elsevier B.V. All rights reserved.
http://dx.doi.org/10.1016/j.bios.2013.08.047

manner (Wilson, 2008). Gold nanoparticles possess distinct physical and chemical properties that make them excellent building blocks for sensor synthesis with outstanding chemical and/or biological attributes (Boisselier and Astruc, 2009; Daniel and Astruc, 2004; Zayats et al. 2005). They possess unique optoelectronic properties, high surface-to-volume ratio and compatibility with numerous functional ligands which make them tunable in responsiveness, such as plasmonic resonance absorption, conductivity, emission spectrum, etc, toward subtle change in surrounding environment (Haick, 2007; Baruah et al. 2012; Nikoobakht and El-Sayed, 2003).

During the last two decades, considerable efforts have been devoted to synthesis of AuNPs, focusing on control over their size, shape, solubility, stability, and functionality, in order to make them excellent probes for different sensing strategies.

Functionalization of AuNPs is currently a "gold standard" necessary for their stability, functionality, and compatibility. For stabilization, AuNPs with molecular coverage of surfactants, such as cetyl trimethylammonium bromide (CTAB), on the surface are essential and widely reported (Chen et al. 2008). Although the stability plays a critical role in preserving functionality, the major goal in functionalization is to maintain the properties of the AuNP and the bound biological molecule. In other words, the biological molecule should be stable and able to retain its biorecognition properties whilst the AuNPs retain their unique properties such as strong plasmon absorption bands (Willets and Van Duyne, 2007).

Past approaches for AuNPs functionalization were pursued with an appropriate biomolecule so that the modified gold nanoprobes undergo structural and functional modifications in order to selectively interact with a target analyte of interest. Subsequently, the interaction of the analyte with functionalized AuNPs (for instance, immunolabeled or DNA coated) produces measurable and quantifiable signals as a result of either an electrochemical/piezoelectric response or a plasmonic shift, for example, the detection of trinitrotoluene (TNT) (Kawaguchi et al., 2008). Despite extensive efforts, it is still a challenge for the fabrication of novel sensors using new design to further achieve sensitive, accurate and facile detection using AuNPs. In addition, the process of functionalized AuNPs is usually complicated, especially ligand binding by antibody (antibodies are usually expensive). The yield of antibody binding is usually not high, and moreover, increases the cost of biosensor. In addition, AuNPs are prone to aggregate and deteriorate sensitivity.

Besides the use of "ligands" for detection specificity, there are a number of intermolecular interactions that can be employed for molecular recognition, such as electrostatic interactions, hydrophobic interactions, hydrogen bonding, covalent bonding, π–π interactions etc (Kim and Kang, 2008; Song et al., 2010). For example, Kim et al. used amine groups to functionalize a given surface making positive charge at neutral pH, they reported that the modified surface was able to interact with negatively charged biomolecules via electrostatic interaction, similar to antibody–antigen interaction. The interaction appears to be specific but limited to charging nature of amine-modified surface.

New approach with facile, cost-effective, and reliable processing is still an ongoing technical niche to be exploited. Here, we present a new colloidal sensing system wherein gold nanorods with clean (or bare) surface were prepared and stabilized on colloidal chitosan nanocarrier. Chitosan, which has been found to be a very useful functional material that possessed the abundant amino groups and gold nanoparticle (GNP) label is an ideal one in biotechnological applications. Zhang et al. designed a chitosan–AuNPs system for electrochemical sensing of human serum albumin (detection range of 8.0–512.0 μg/mL) (Zhang et al., 2007). Lim and Kang disclosed a sensing device that could quickly sense dopamine concentration by using chitosan–gold nanoshell and claimed that the detection range of dopamine was from 1 to 10 mM by surface-enhanced Raman scattering (Lim and Kang, 2013). AuNPs–chitosan composite films were designed as sensitive and selective electrochemical sensors for detection of caffeic acid (achieving with a detectable range of 5.00×10^{-8} M–2.00×10^{-3} M). Moreover, chitosan free amino groups can be responsible for an electrostatic interaction with the carboxylic group of the caffeic acid (Carlo et al., 2012).

Upon a subtle manipulation of electrostatic interactions between the bare-surfaced Au nanorods, colloidal chitosan carrier, and protein molecules, the sensitivity and selectivity for specific proteins, i.e., human serum albumin and lysozyme used as model molecules, for the first time, can be accurately monitored at a picomolar level using a conventional UV–vis spectroscopy without employing specific receptor/antibody on the bare Au surface.

2. Experimental procedures

2.1. Materials

$HAuCl_4\cdot3H_2O$, $AgNO_3$, $NaBH_4$, ethanol (99.8%) and buffer solutions (pH 4, 9 and 10) were purchased from Sigma Aldrich. Cetyl trimethylammonium bromide (CTAB), buffer solutions (pH 5 and 8) were purchased from Alfa Aesar. L-ascorbic acid (LAA, 99%) was purchased from J.T. Baker. Chitosan polymer was purchased from Advanced Delivery Technology Co. (molecular weight is 210,000, de-acetylation degree is 91.3%, Taiwan) The proteins, lysozyme from chicken egg white (Lys.) and albumin from human serum (HSA) were purchased from Sigma Aldrich and used without further purification. All the solutions were prepared with ultrapure deionized water (DI water), and all the glasswares were cleaned thoroughly with DI water before the experiments.

2.2. Synthesis of AuNRs

The AuNRs colloid we used was prepared by seed-mediated growth procedure. First, a gold seed solution was prepared by reduction of $HAuCl_4$ (5 mL, 5×10^{-4} M) with $NaBH_4$ (0.6 mL, 0.1 M) in the presence of CTAB (5 mL, 0.2 M) under stirring condition. After 1.5 h, the reaction was finished at 35 °C and solution color gradually turned into brownish-yellow appearance. This brownish-yellow solution was used for the synthesis of AuNRs. Upon the synthesis, 2.5 mL of 0.01 M $HAuCl_4$ was mixed with 47.5 mL of 0.1 M CTAB and 0.6 mL of 0.01 M silver nitrate aqueous solution. After gentle mixing of the solution, 0.275 mL of 0.1 M LAA was gradually added with continuously stirring, and then 0.06 mL of seed solution was finally added into the mixture. The AuNRs was formed when the solution color was changed. These AuNRs were aged for 24 h under stirring, and then the excess CTAB was removed by centrifugation.

2.3. Synthesis of AuNR@CHC colloids

First, 0.9 mL of DI water was added to 0.1 mL of the prepared AuNR solution and centrifugation at 7000 rpm for 15 min. Second, 0.1 mL of CHC solution was added to the above solution, and using 0.9 mL of ethanol to remove CTAB from AuNRs surface. Third, the ethanol supernatant was removed from the solution under centrifuged at 12,000 rpm for 20 min. The gel-like AuNR–CHC NPs were formed and then 1 mL of DI water was added to re-disperse the gel-like AuNR–CHC NPs to form a well-suspended solution. Finally, the obtained solution from 0.5 mL of AuNR–CHC solution was mixed with 0.5 mL of various buffer solutions, as used for UV–vis monitoring. In a calculation, we estimated that there has

Table 1
Calculation estimate on the numbers of AuNRs and colloidal chitosan that can be produced under experimental control. The number of AuNRs deposited on a given single chitosan colloid was also estimated, which is closed to what was detected using TEM observation.

Est. number of AuNRs in the solution	Est. number of chitosan colloids formed in the solution	Average number of AuNRs on chitosan colloids after electrostatic deposition in the mixed solution
7.7×10^{10}	2.4×10^{10}	3.2

about 3 AuNRs deposited on a single CHC colloidal nanoparticle, the results are listed in Table 1.

2.4. Analysis

The absorption spectra were obtained by the UV–vis spectrophotometer (Thermo Scientific Evolution 3000, USA). The quartz cell was used before the measurement that was cleaned by soaking in aqua regia and then washed with DI water and ethanol. Every test condition was measured three times by individual samples. The results were averaged by three measured data. The UV–vis measurements were started after 5 min by the addition of HSA or Lys. proteins. Zeta potentials were determined to get information on the net charge of the varied materials. The pH was adjusted from 4 to 10 using a phosphate buffer solution. Zeta potentials were measured with a Delsa Nano C (Beckman Colter, U.S.A.), which uses photon correlation spectroscopy of incident laser light. The Raman spectra were measured on Horiba Jobin Yvon LabRAM HR800 Raman Microscope. TEM EDS mapping was performed in a FEI Tecnai Osiris TEM/STEM, operated at 200 kV. The TEM/STEM is equipped with 4 windowless SDD EDS detectors, which make EDS mapping work more efficient and minimize the effect of specimen drift.

3. Results and discussion

3.1. Effect of AuNR aspect ratio on UV–vis spectral shift

Gold nanorods (AuNRs) are of particular interest due to their unique SPR behavior. In Fig. 1, the UV–vis spectra exhibit a clear evidence on the spectral shift of the AuNRs with different aspect ratios, wherein the spectral shift becomes large while the aspect ratio increases. In sensing application, the larger spectral shift translated a better resolution toward a given concentration of the analyte, and it is frequently realized to have as low as possible analyte concentration, i.e., lower limit of detection, such as in picomolar to femtomolar resolution (García et al., 2010; Sagle et al., 2011; Cottat et al., 2013). Therefore, the AuNRs with the aspect ratio of 5.2 were employed for subsequent study.

3.2. Bare gold nanorods with improved detection sensitivity

Experimental observation indicated that stabilization of the bare-surfaced AuNRs in the presence of positively-charged CHC colloids was achieved, comparing to a rapid agglomeration (a rapid color change was observed) of the nanorods in CHC-free solution, right after CTAB was washed away. Such a stabilization was due to a rapid deposition of the negatively-charged bare AuNRs on the positively-charged surface of CHC colloids, which ensures the stability for the resulting AuNR–CHC nanosuspesion, in the meantime, prevents the bare AuNRs from agglomeration, is given in Fig. 2a. The bare-surfaced AuNRs may be more beneficial toward a response of the analyte molecule by providing a pronounced spectral shift of the SPR spectrum even at a relatively

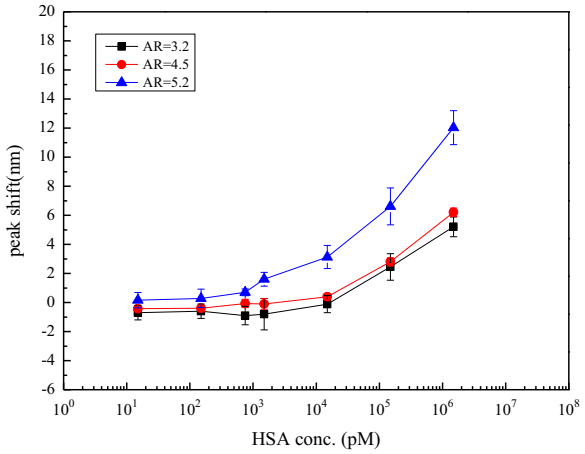

Fig. 1. The UV–vis peak shift versus HSA concentration for the AuNRs of various aspect ratios.

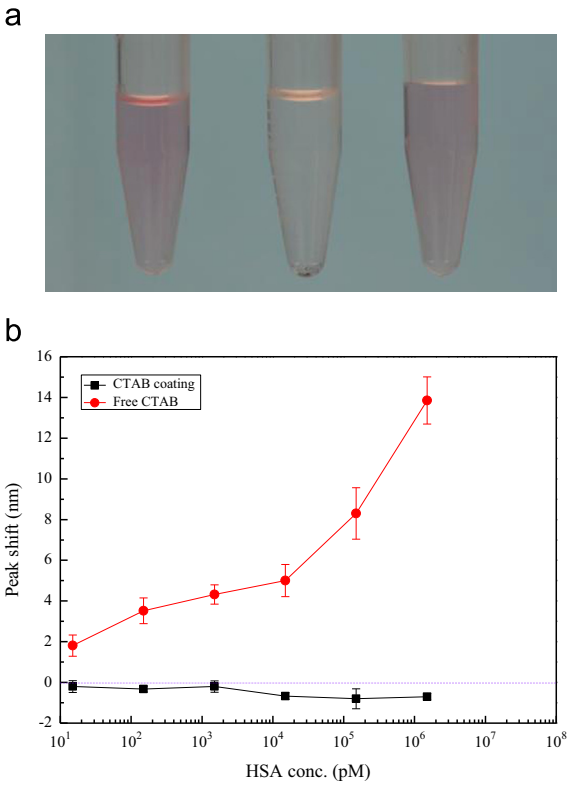

Fig. 2. (a) The appearance of the solutions: left—CTAB-stabilized AuNR suspension; middle—CTAB-free AuNR suspension where the AuNRs were settled down to the bottom of the vial; right—CTAB-free AuNRs in the presence of CHC colloids, showing a well-stabilized suspension. (b) A comparison of detection capability on human serum albumin (HSA) between CTAB-stabilized and CTAB-free AuNRs.

low concentration, compared to the surface covered with a layer of surfactant, such as CTAB. Using human serum albumin (HSA) as model molecule, where the bare-surfaced AuNRs give much better spectral resolution over a wide range of concentrations, even to a trace amount of 15 pM, using conventional UV–vis spectroscopy, as shown in Fig. 2b. This finding also ensures a considerable improvement of the detection limit for bare-surfaced AuNRs, in other words, an enormous enhancement of sensitivity and detection stability compared to those CTAB-stabilized AuNRs can be achieved (Saha et al., 2012).

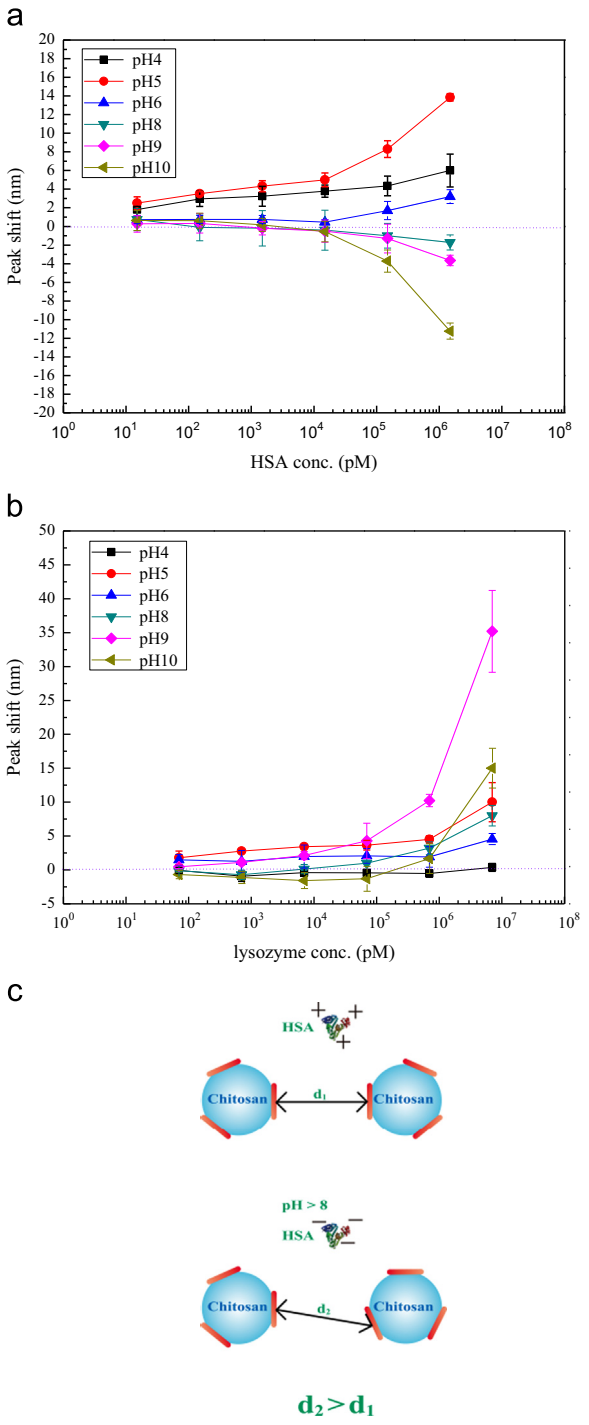

Fig. 3. The UV–vis peak shift with different pH values for (a) HSA and (b) lysozyme. (c) Schematic presentation on a blue-shift mechanism due to an increased AuNR-AuNR repulsion upon depletion stabilization in the presence of non-adsorbed proteins among CHC–AuNR colloids.

3.3. *Electrostatically-induced selectivity*

Evaluation on the spectral resolution for the AuNR–CHC colloids in terms of different pH values, from pH 4 to pH 10, is given in Fig. 3a and b for HSA and lysozyme, respectively. For HSA, spectral shift exhibited a wide variety of profiles from blue shift at solution pH $\geq$ 8 to red shift at pH $\leq$ 6. Accordingly, the red-shift profile, indicating a reduction of surface energy of the AuNR, is mainly contributed as a result of HSA adsorption or colloidal aggregation. However, blue-shift profiles were enlarged with increasing HSA concentration. Accordingly, blue-shift effect is indicative of an enhanced plasmonic resonance of Au nanoparticle which is associated with an increased surface energy of the particles (Johan et al., 2012). Previous studies on monitoring the distance between two adjacent Au nanoparticles concluded that the blue shift in SPR spectrum is originated from an increased separation between Au nanoparticles (Rechberger et al., 2003; Wang and Yu, 2010). This may explain the blue-shift behavior in Fig. 3a, where at pH > 8, both HSA and AuNR (deposited on CHC colloidal carrier) were highly negatively charged, e.g., about −15 mV and −50 mV at pH=10, respectively, the HSA turns to be a non-adsorbed species distributed freely in the colloidal suspension. The resulting blue-shift spectra for the AuNRs suggested a further separation of the AuNRs between AuNR–CHC colloids due to a possible mechanism of depletion stabilization, as schematically proposed in Fig. 3c.

However, for the case of lysozyme, Fig. 3b shows no blue-shift effect over the whole range of lysozyme concentration studied, especially at pH > 8, compared to the case of HSA in Fig. 3a. Since the IEP for the lysozyme is 9.3, a change from slightly positive charge to slightly negative charge of the lysozyme can be expected from pH=9 to pH=10, wherein a deposition toward AuNR is expected for the former, whilst a major deposition onto CHC matrix was more likely to dominate for the latter.

However, what is most critically important to be emphasized in this investigation is that at a given HSA concentration, the largest spectral shift was detected at pH=5.0, a value close to the IEP of HSA (which is determined to be 5.02 in this study). Similar behavior was observed for lysozyme, Fig. 3b, where the largest spectral shift at a given concentration is at pH=9, which is slightly lower than its IEP value, i.e., pH=9.3 determined experimentally.

Fig. 3 also discloses an excellent detection limit to a value as low as 1 ng/mL of the proteins, corresponding to 70 pM for lysozme and 15 pM for HSA, which is hardly accessible from prior detecting protocols using Au nanoparticles (Zhang et al., 2007; Wang and Yu, 2010). In fact, advanced spectroscopic apparatuses, such as surface-enhanced Raman spectroscopy, dynamic light scattering, and fluorescence quenching, have been frequently employed as important analytical tools for surface plasmonic nanosensors (Liu et al., 2008; Dasary et al., 2009; Cheng et al., 2011), in order to achieve the highest detection resolution, e.g., at a LOD range from nanomolar to femtomolar level. Comparing to current experimental observation, it is more interesting and practically important to utilize the AuNR–CHC colloid as sensor, since it provides an excellent molecular resolution comparable to existing Au-based nanosensors, in the meantime, a reasonably high sensitivity can be easily determined via a simple and affordable UV–vis facility.

A closer look at the pH-dependent spectral shift for both proteins in Fig. 3 suggests that solution pH is acting as an essential role in detecting specificity, since the highest detecting resolution was at a pH level closed to the IEP of the protein itself. This finding strongly implies a specific interaction dominating the adsorption behavior between AuNR and protein. To further confirm the adsorption specificity, we examine two samples with HSA using EDAX mapping as displayed in Fig. 4a and b, for the detection at pH=5 and pH=9, respectively. It is relatively clear that at pH 5, the mapping profile of the sulfur, an important characteristic element in HSA, (in red-color appearance) shows the HSA being highly preferentially deposited on the AuNR surface, whilst at pH 9, the HSA is randomly distributed mostly on the CHC surface. The elemental mapping also agreed with the spectral shift illustrated in Fig. 4a. This interesting finding appears to substantiate a highly selective sensing capability that can be optimized using a synergistic control between solution pH and the charging variation of the AuNR–CHC colloids.

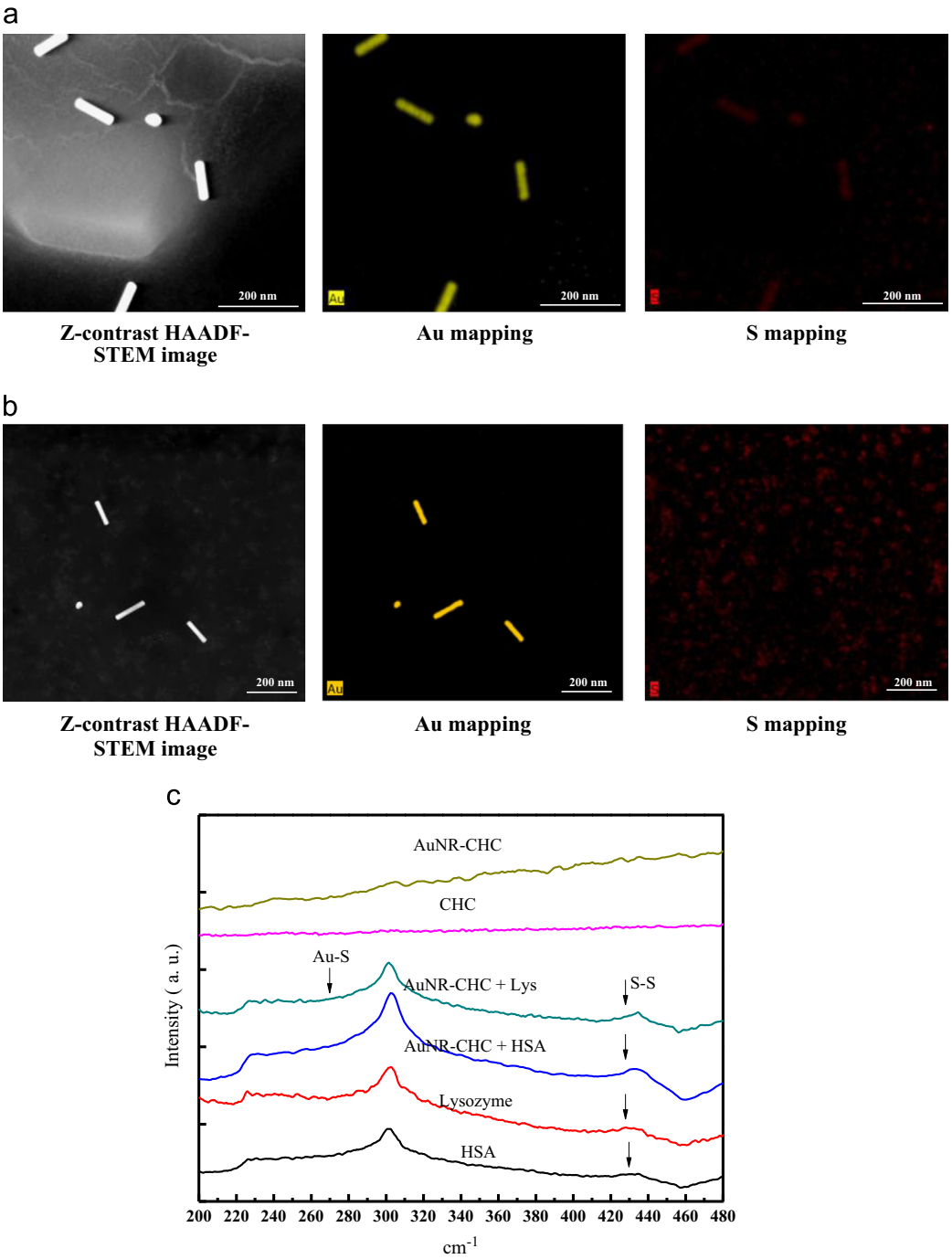

Fig. 4. TEM photos and chemical mapping images for 150 nM HSA measured at (a) pH=5 and (b) pH=9, showing a clear site-specific deposition on AuNRs surface (s mapping) at pH=5, but turns to be relatively non-specific at pH=9.0. (c) The Raman spectra of the chitosan–AuNR and proteins, wherein no signal of Au–S characteristic absorption peak was observed. (For interpretation of the references to color in this figure legend, the reader is referred to the web version of this article.)

In the meantime, Raman spectral analysis on the sample with HSA or lysozyme preferentially deposited on the AuNRs shows no Au–S stretching signal at ~270 nm(Mikhlin et al., 2009), as depicted in Fig. 4c, suggesting that the preferential deposition is unlikely to be driven through the covalent affinity between Au and S. This finding provides a supporting cue of electrostatically-induced protein-specific interaction with the AuNRs on the colloids.

3.4. The mechanism of pH-mediated detection specificity

To impart a high selectivity to conventional sensing probes, a preferential interaction between the target analyte and molecular probe has to be highly specified. This is the major rationale to integrate specific ligands such as antibody, peptides, proteins, etc. on a signal transducer for biomarker detection in all kinds of Au plasmonic-based sensing devices (De et al., 2008). However, a new approach proposed for the first time from current study, over which a subtle manipulation of zeta potential between proteins and AuNR–CHC colloids via control of solution pH may achieve desirable sensing selectivity, without acquiring specific "ligands" for recognition purpose.

Associated with the pH-dependent spectral shift profiles and mapping profiles for both HSA and lysozyme selectively shown in Figs. 3 and 4, we propose a mechanism, as illustrated in Fig. 5a, that enables our understanding on the specific interaction, which

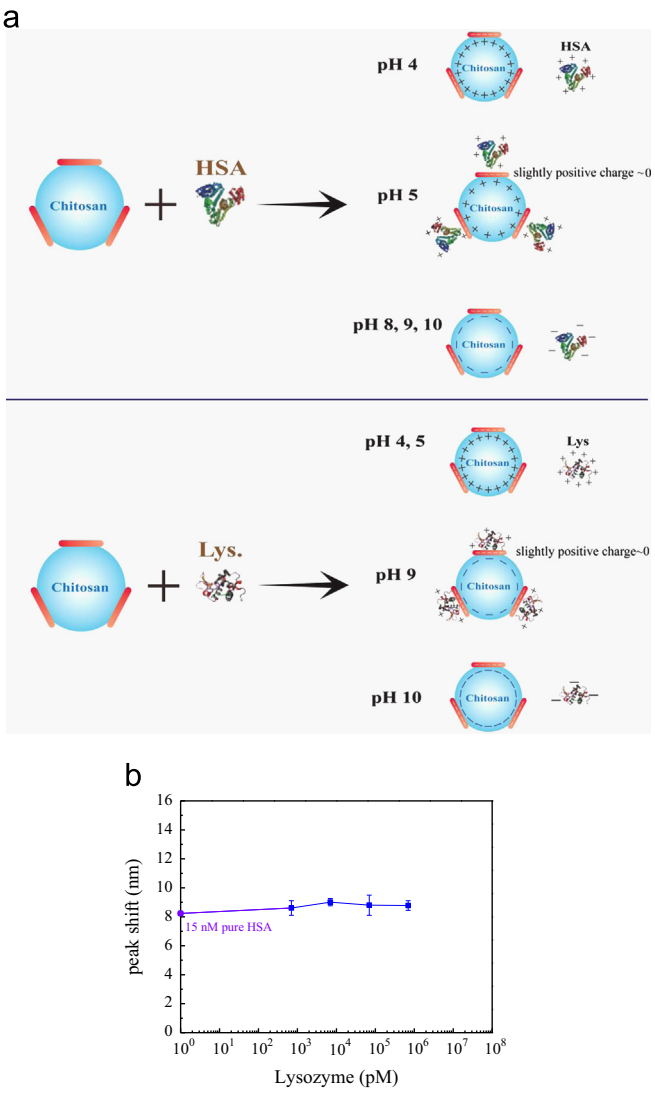

Fig. 5. (a) The mechanism proposed for the sensing selectivity derived from a manipulation of electrostatic interactions between colloidal nanoprobe, protein, and solution pH. (b) The UV–vis peak shift with 15 nM HSA remains relatively constant (the same spectral shift as that for pure HSA of identical concentration at pH=5) in the presence of various concentrations of lysozyme, suggesting detection specificity can be achieved upon the subtle control of solution pH.

can also translate as a function of sensing specificity using current AuNR–CHC colloids, for HSA and lysozyme. In the case of HSA, when solution pH is closed to its IEP, i.e., pH=5.0, a strong electrostatic attraction between negatively-charged AuNRs and HSA (bearing ~zero or slightly positive charge), while in the meantime, CHC surface is highly positively-charged, rendering a highly preferential deposition. However, for solution pH > 5, charge nature of the CHC colloids may transfer from less positive where the attraction force turned to be weaker, to zero (at pH=7.5) and negative sign (at pH between 7.5 and 8.5), where colloidal instability deteriorated the detection ability. At pH=10, stronger electrostatic repulsion between AuNRs and HSA (turned to be negatively charged) deteriorates the preferential deposition. For the case of lower solution pH, i.e., at 4, AuNRs bear a positive charge, resulting in a repulsion toward the positively-charged HSA.

Similar scenario can be applicable to lysozyme, having an IEP=9.3, determined experimentally. At solution pH=9, a strong electrostatic attraction dominates the preferential deposition, giving the highest specificity toward lysozyme deposition. However, further increase solution pH to 10, negatively-charged lysozyme exerted a repulsive force toward the AuNRs, rendering a poor adsorptive specificity. At solution pH < 8.0, a region where colloidal instability deteriorated the detection resolution and specificity. In a more acidic region between pH 6 and 4, electrostatic repulsion between AuNRs and positively-charged lysozyme caused a poor site-specific deposition.

3.5. Detection specificity from protein mixture

To demonstrate detection selectivity of current colloidal nanoprobes based on the mechanism proposed in Fig. 5a, a mixture of HSA and lysozyme was prepared and measured by UV–vis at pH=5. Fig. 5b shows the resulting spectral shift of the HSA in the presence of various lysozyme concentrations. Comparing with the spectral shift for pure HSA, the presence of various concentrations of lysozyme showed no appreciable influence on the resulting spectral shift, suggesting a highly detection specificity for the HSA can be well manipulated. According to the proposed mechanism, the HSA would preferentially deposit on AuNRs surface whilst lysozyme was repelled away from CHC, resulting in a nice demonstration of detection specificity.

In short, an optimized sensing capability for the AuNR–CHC colloidal probe can be manipulated upon a subtle control over the solution pH closed to the IEP of the target proteins, over which a highly preferential deposition of the protein toward the bare AuNRs on the CHC substrate can be achievable. This study also reveals the feasibility to turn originally non-specific electrostatic interactions into more specific nature upon a precise manipulation of the colloidal properties included charge, stability, and buffer pH, among CHC nanocarrier, bare Au nanorods, and the proteins to be monitored. Similar design rationale may be deduced from this study by a synergistic combination between various colloidal nanocarrier and solution pH, for detecting a wide variety of proteins with high sensitivity and recognition.

4. Conclusion

In summary, deposition of a few bare-surface Au nanorods with AR=5.2 on positively-charged colloidal chitosan carrier has gained significant analytical resolution toward specific proteins, i.e., human serum albumin and lysozyme, at a picomolar precision via conventional UV–vis spectroscopy. Control of solution pH at a value closed to isoelectric point of the proteins, i.e., pH=5 for HSA and pH=9 for lysozyme in this study, leads to a highly preferential deposition toward the bare-surfaced AuNRs, rather than on the CHC colloidal surface, as a result of electrostatically-driven site-specific adsorption. This renders a high sensing selectivity for the colloid-type AuNR–CHC nanosensor to be technically accessible for a wide range of analytical applications, without acquiring any ligands.

References

Baruah, B., Craighead, C., Abolarin, C., 2012. Langmuir 28 (43), 15168–15176.
Boisselier, E., Astruc, D., 2009. Chemical Society Reviews 38, 1759–1782.
Carlo, G.D., Curulli, A., Toro, R.G., Bianchini, C., Caro, T.D., Padeletti, G., Zane, D., Ingo, G.M., 2012. Langmuir 28 (12), 5471–5479.
Chen, A., Chatterjee, S., 2013. Chemical Society Reviews 42 (12), 5425–5438.
Chen, P.C., Mwakwari, S.C., Oyelere, A.K., 2008. Nanotechnology, Science and Applications 1, 45–66.
Cheng, Y., Stakenborg, T., Dorpe, P.V., Lagae, L., Wang, M., Chen, H., Borghs, G., 2011. Analytical Chemistry 83, 1307–1314.
Cottat, M., Thioune, N., Gabudean, A.M., Lidgi-Guigui, N., Focsan, M., Astilean, S., de la Chapelle, M.L., 2013. Plasmonics 8 (2), 699–704.
Cui, R.J., Liu, C., Shen, J.M., Gao, D., Zhu, J.J., Chen, H.Y., 2008. Advanced Functional Materials 18, 2197–2204.
Daniel, M.C., Astruc, D., 2004. Chemical Reviews 104, 293–346.

Dasary, Samuel S.R., Singh, A.K., Senapati, D., Yu, H., Ray, Paresh C., 2009. Journal of the American Chemical Society 131 (38), 13806–13812.
De, M., Ghosh, P.S., Rotello, V.M., 2008. Advanced Materials 20, 4225–4241.
Doria, G., Conde, J., Veigas, B., Giestas, L., Almeida, C., Assunção, M., Rosa, J., Baptista, P.V., 2012. Sensors 12, 1657–1687.
García, M.A., Bouzas, V., Carmona, N., 2010. AIP Conference Proceedings, vol. 1275. pp. 84–87.
Haick, H., 2007. Journal of Physics D: Applied Physics 40, 7173–7186.
Johan, M.R., Chong, L.C., Hamizi, N.A., 2012. International Journal of Electrochemical Science 7, 4567–4573.
Kawaguchi, T., Shankaran, D.R., Kim, S.J., Matsumoto, K., Toko, K., Miura, N., 2008. Sensors and Actuators B: Chemical 133, 467–472.
Kim, D.C, Kang, D.J., 2008. Sensors 8, 6605–6641.
Lei, J., Ju, H., 2012. Chemical Society Reviews 41, 2122–2134.
Lim, J.W., Kang, I.J., 2013. Bulletin of the Korean Chemical Society 34 (1), 237–242.
Liu, X., Dai, Q., Austin, L., Coutts, J., Knowles, G., Zou, J.H., Chen, H., Huo, Q., 2008. Journal of the American Chemical Society 130 (9), 2780–2782.
Mikhlin, Y., Likhatski, M., Karacharov, A., Zaikovskib, V., Krylovc, A., 2009. Physical Chemistry Chemical Physics 11, 5445–5454.
Nikoobakht, B., El-Sayed, M.A., 2003. The Journal of Physical Chemistry A 107, 3372–3378.
Rechberger, W., Hohenau, A., Leitner, A., Krenn, J.R., Lamprecht, B., Aussenegg, F.R., 2003. Optics Communications 220, 137–141.
Sagle, B., Ruvuna, L.K., Ruemmele, J.A., Van Duy, R.P., 2011. Nanomedicine 6 (8), 1447–1462.
Saha, K., Agasti, S.S., Kim, C., Li, X., Rotello, V.M., 2012. Chemical Reviews 112, 2739–2779.
Song, H.D., Choi, I., Yang, Y.I., Hong, S., Lee, S., Kang, T., 2010. Yi. Journal of Nanotechnology 21, 145501.
Tansil, N.C., Gao, Z.Q., 2006. Nano Today 1, 28–37.
Wang, B., Yu, C., 2010. Angewandte Chemie International Edition 49, 1485–1488.
Willets, K.A., Van Duyne, R.P., 2007. Annual Review of Physical Chemistry 58, 267–297.
Wilson, R., 2008. Chemical Society Reviews 37, 2028–2045.
Wu, Y.F., Chen, C.L., Liu, S.Q., 2009. Analytical Chemistry 81, 1600–1607.
Yu, X., Munge, B., Patel, Y., Jensen, G., Bhirde, A., Gong, J.D., Kim, S.N., Gillespie, J., Gutkind, J.S., Papadimitrakopoulos, F., Rusling, J.F., 2006. Journal of the American Chemical Society 128, 11199–11205.
Zayats, M., Baron, R., Popov, I., Willner, I., 2005. Nano Letters 5, 21–25.
Zhang, S.B., Wu, Z.S., Guo, M.M., Shen, G.L., Yu, R.Q., 2007. Talanta 71, 1530–1535.